

# Antiferromagnetic Heisenberg chains with bond alternation and quenched disorder

Yu-Cheng LIN<sup>1</sup>, Heiko RIEGER<sup>2</sup> and Ferenc IGLÓI<sup>3,4</sup>

<sup>1</sup> *Institut für Physik, WA 331, Johannes Gutenberg-Universität, 55099 Mainz, Germany*

<sup>2</sup> *Theoretische Physik, Universität des Saarlandes, 66041 Saarbrücken, Germany*

<sup>3</sup> *Research Institute for Solid State Physics and Optics, H-1525 Budapest, P.O.Box 49, Hungary*

<sup>4</sup> *Institute of Theoretical Physics, Szeged University, H-6720 Szeged, Hungary*

We consider  $S = 1/2$  antiferromagnetic Heisenberg chains with alternating bonds and quenched disorder, which represents a theoretical model of the compound  $\text{CuCl}_{2x}\text{Br}_{2(1-x)}(\gamma - \text{pic})_2$ . Using a numerical implementation of the strong disorder renormalization group method we study the low-energy properties of the system as a function of the concentration,  $x$ , and the type of correlations in the disorder. For perfect correlation of disorder the system is in the random dimer (Griffiths) phase having a concentration dependent dynamical exponent. For weak or vanishing disorder correlations the system is in the random singlet phase, in which the dynamical exponent is formally infinity. We discuss consequences of our results for the experimentally measured low-temperature susceptibility of  $\text{CuCl}_{2x}\text{Br}_{2(1-x)}(\gamma - \text{pic})_2$ .

**KEYWORDS:**  $\text{CuCl}_{2x}\text{Br}_{2(1-x)}(\gamma - \text{pic})_2$ , low-temperature susceptibility, random Heisenberg chain, correlated disorder, strong disorder renormalization group, random singlet phase, quantum Griffiths phase

## 1. Introduction

Low-dimensional quantum systems (antiferromagnetic spin chains, ladders, two-dimensional systems, etc.) are fascinating objects which have been investigated intensively in experimental and theoretical works. From the theoretical point of view these systems exhibit several unusual properties, for example quasi-long-range order, topological string order, a spin liquid state, quantum phase transitions, etc.. Many of these features can be illustrated by the  $S = 1/2$  antiferromagnetic Heisenberg chain, which is defined by the Hamiltonian:

$$H = \sum_i 2J_i \mathbf{S}_i \cdot \mathbf{S}_{i+1}, \quad (1)$$

in terms of the spin-1/2 operators,  $\mathbf{S}_i$ , at site  $i$ . The homogeneous model with  $J_i = J$  is gapless and there is quasi-long-range order in the ground state, i.e. spin-spin correlations decay algebraically,<sup>1</sup>  $\langle S_i^\tau S_{i+r}^\tau \rangle \sim r^{-1}$ . Here  $\tau = x, y, z$  and  $\langle \dots \rangle$  stands for the ground-state expectation value. Introducing bond alternation such that  $J_i = J$  at  $i = \text{even}$  and  $J_i = \alpha_d J$ , ( $\alpha_d > 0$ ) at  $i = \text{odd}$ , the system with  $\alpha_d \neq 1$  is in the dimerized phase,<sup>2</sup> in which spin-spin correlations are short-ranged and the excitation spectrum has a finite gap. In the bond alternating model the quantity  $\delta_d = \ln \alpha_d$  serves as a quantum control parameter and the quantum critical point is located at  $\delta_d^c = 0$ .

Quenched (i.e. time independent) disorder has a profound effect on the low-temperature/low-energy properties of quantum systems,<sup>3</sup> both at the quantum critical point and in an extended region of the off-critical regime—the so called quantum Griffiths phase.<sup>4,5</sup> In the disordered version of the uniform  $S = 1/2$  antiferromagnetic Heisenberg chain defined in eq.(1), the couplings,  $J_i$ , are independent and identically distributed random variables. A detailed study by Fisher<sup>6</sup> using

an asymptotically exact strong disorder renormalization group (SDRG) method<sup>7</sup> revealed that the ground state of the random model is the so called random singlet phase, in which singlets are formed between spin pairs which could be arbitrarily far apart. Average spin-spin correlations, which are dominated by rare regions, are quasi-long-ranged:  $[\langle S_i S_{i+r} \rangle]_{\text{av}} \sim r^{-2}$ , where  $[\dots]_{\text{av}}$  stands for averaging over quenched disorder. On the other hand, *typical* correlations are much weaker and decay asymptotically as  $\ln(\langle S_i S_{i+r} \rangle_{\text{typ}}) \sim r^{1/2}$ . In addition, the dynamical scaling in the random singlet phase is anomalous. The length scale  $L$  and the energy scale  $\Delta$ , measured by the lowest gap, are related logarithmically:

$$\ln \Delta \sim L^\psi, \quad \psi = 1/2. \quad (2)$$

In the random bond alternating Heisenberg model bonds at even ( $J_e$ ) and odd ( $J_o$ ) sites are taken from different distributions and the quantum control parameter is defined as

$$\delta = [\ln J_e]_{\text{av}} - [\ln J_o]_{\text{av}}. \quad (3)$$

For  $\delta \neq 0$  the model is in the random dimer phase, in which spatial spin-spin correlations are short ranged.<sup>8</sup> Within a range of finite dimerization  $|\delta| < \delta_G > 0$ , dynamical correlations are however still quasi-long-ranged, which is related to the fact that the system is gapless. This region is called Griffiths phase. In a finite chain of length  $L$  the typical gap scales asymptotically as:

$$\Delta \sim L^{-z}. \quad (4)$$

Here the dynamical exponent,  $z$ , is a continuously varying function of the control parameter,  $\delta$ . On the border of the Griffiths phase,  $\delta = \delta_G$ , the dynamical exponent vanishes, whereas close to the random singlet phase it diverges with  $\delta \rightarrow 0$  as:<sup>6</sup>

$$z \sim 1/\delta. \quad (5)$$

In the random singlet phase as well as in the Griffiths phase, thermodynamic quantities such as the low-temperature susceptibility,  $\chi(T)$ , the low-temperature specific heat,  $C(T)$ , and the low-field magnetization,  $M(h)$ , at zero temperature are singular. For example the susceptibility in the random singlet phase behaves as:

$$\chi(T) \sim \frac{1}{T(\ln T)^2}, \quad (6)$$

whereas in the Griffiths phase it is given by:

$$\chi(T) \sim T^{-1+\beta}, \quad \beta = 1/z. \quad (7)$$

Recent experimental studies on the compound  $\text{CuCl}_{2x}\text{Br}_{2(1-x)}(\gamma - \text{pic})_2$  show another type of competition between bond alternation and randomness.<sup>9,10</sup> Here the  $x = 0$  compound,  $\text{CuBr}_2(\gamma - \text{pic})_2$ , is a homogeneous  $S = 1/2$  antiferromagnetic Heisenberg chain in which the Cu – Cu bond is bi-bridged by two Br atoms:  $\text{Cu} < \begin{smallmatrix} \text{Br} \\ \text{Br} \end{smallmatrix} > \text{Cu}$  and the coupling constant is given by  $J'' = 20.3\text{K}$ .<sup>9</sup> The  $x = 1$  compound,  $\text{CuCl}_2(\gamma - \text{pic})_2$ , is a bond alternating  $S = 1/2$  antiferromagnetic Heisenberg chain in which two kinds of  $\text{Cu} < \begin{smallmatrix} \text{Cl} \\ \text{Cl} \end{smallmatrix} > \text{Cu}$  bonds alternate along the chain.<sup>11</sup> The bond alternation is induced by a freezing transition of the rotational motion of the methyl-group at  $50\text{K}$ .<sup>11</sup> The experimentally measured coupling strengths are  $J = 13.2\text{K}$  and  $J\alpha$ , with  $\alpha = 0.6$ . In the mixed compound with a small finite concentration of Br ( $x \neq 1$ ), atoms connected with alternating  $\text{Cu} < \begin{smallmatrix} \text{Cl} \\ \text{Cl} \end{smallmatrix} > \text{Cu}$  bonds form a cluster and different clusters are separated by bonds with Br – Br and/or Br – Cl bridges. The strength of the  $\text{Cu} < \begin{smallmatrix} \text{Br} \\ \text{Cl} \end{smallmatrix} > \text{Cu}$  bond has been estimated from the theoretically calculated magnetization curve as  $J' = 1.3J$ .<sup>12</sup> In ref. 9 the data for the low-temperature susceptibility of the diluted system show an algebraic temperature dependence,  $\chi \sim T^{\beta-1}$ , which is compatible with the expected behavior in the Griffiths phase as given by eq.(7). For a wide range of the concentration,  $x$ , the measured effective exponent is about  $\beta_{\text{exp}} \approx 0.5 - 0.67$ , and shows only a weak concentration dependence.

## 2. Theoretical Model

A theoretical model for  $\text{CuCl}_{2x}\text{Br}_{2(1-x)}(\gamma - \text{pic})_2$  was presented and numerically studied in ref. 12. It is not obvious from the information one can extract from the experiments whether the rotational order of the methyl-group remains long-ranged in the presence of the dilution by  $\text{Cu} < \begin{smallmatrix} \text{Br} \\ \text{Cl} \end{smallmatrix} > \text{Cu}$  or  $\text{Cu} < \begin{smallmatrix} \text{Br} \\ \text{Br} \end{smallmatrix} > \text{Cu}$ . Therefore two models were introduced in:<sup>12</sup> i) The *fixed parity* model in which the rotational order is assumed to be perfectly long ranged, i.e. the  $J$  ( $\alpha J$ ) bonds stay in the same parity position, say at  $i = \text{even}$  ( $i = \text{odd}$ ), in any bond-alternating cluster. Introducing a parity parameter,  $p_i$ , given by  $p_i = 1(-1)$  if the  $\text{Cu} < \begin{smallmatrix} \text{Cl} \\ \text{Cl} \end{smallmatrix} > \text{Cu}$  bond has a value of  $J$  ( $\alpha J$ ), one can describe the parity correlations in the fixed parity model as  $p_i p_{i+2l} = 1$  and  $p_i p_{i+2l-1} = -1$ ; ii) The *random parity* model in which the rotational long-range order between two clusters of alternating bonds is assumed to be completely destroyed by the dilution. In this case, if  $i$  and  $i + 2l$  ( $i + 2l - 1$ ) refer to different clusters, the average parity correlations

vanish:  $[p_i p_{i+2l}]_{\text{av}} = [p_i p_{i+2l-1}]_{\text{av}} = 0$ .

In this paper we consider a more general model in which rotational long-range order is partially destroyed by dilution, so that correlations between parities in two different clusters are given asymptotically as  $[p_i p_{i+2l}]_{\text{av}} = -[p_i p_{i+2l-1}]_{\text{av}} \sim l^{-\rho}$ . Here we recover the fixed parity and the random parity models in the limits  $\rho = 0$  and  $\rho \rightarrow \infty$ , respectively. We note that some aspects of the effect of correlated disorder on quantum systems is studied in ref. 13. Here we summarize the values of the coupling constant in eq.(1) in the following way:

$$J_i = \begin{cases} J\alpha^{(1-p_i)/2} & \text{with prob. } x^2 \\ J' & \text{with prob. } 2x(x-1) \\ J'' & \text{with prob. } (x-1)^2 \end{cases} \quad (8)$$

The parity correlations within a cluster of alternating bonds are given by  $p_i p_{i+j} = (-1)^j$  and the parity correlations for bonds in different clusters are defined above for the different models.

The theoretical results for the low-energy behavior of the fixed parity and the random parity models obtained from the density matrix renormalization group (DMRG) method<sup>12</sup> are not fully consistent with the measured low-temperature properties of the  $\text{CuCl}_{2x}\text{Br}_{2(1-x)}(\gamma - \text{pic})_2$ .<sup>9</sup> In ref. 12 the random parity model is found to be in the random singlet phase, in which the susceptibility exponent is  $\beta = 0$  and is much lower than the experimental value  $\beta_{\text{exp}} \approx 0.5 - 0.67$ . For the fixed parity model the susceptibility exponent is found to be too large:  $\beta \geq 1$ . Another problem with the latter model is that the DMRG analysis could not be performed for  $x \leq 0.4$  due to strong finite size effects.

In the present paper we revisit the models of the compound  $\text{CuCl}_{2x}\text{Br}_{2(1-x)}(\gamma - \text{pic})_2$ . Our study is different from ref. 12 in two respects. Firstly, we consider a more general model in which the effect of disorder correlations are taken into account. Secondly, we use a numerical implementation of the SDRG method. This method usually gives very accurate results for the form of singularities, in particular for the dynamical exponent.<sup>14</sup> This method has been successfully applied to clarify the low-energy singularities of more complicated systems, such as random spin ladders<sup>15</sup> and two- and three-dimensional random Heisenberg antiferromagnets.<sup>16</sup> The major advantage of this method is that one can consider large systems  $L \sim 1000 - 2000$  with good statistics compared with the DMRG method.

## 3. Numerical results

### 3.1 Numerical method

The SDRG method for random AF spin chains proceeds as follows: During the renormalization process, one first identify the strongest bond, say  $J_{23} = \Omega$ , which connects sites 2 and 3. If the neighboring bonds are much weaker,  $J_{23} \gg J_{12}, J_{34}$ , then the spins 2 and 3 form an effective singlet and can be decimated out. The new coupling between the remaining sites, 1 and 4, is obtained

within a second-order perturbation calculation as:

$$\tilde{J} = \frac{1}{2} \frac{J_{12} J_{34}}{J_{23}}. \quad (9)$$

By repeating this decimation process, we gradually reduce the energy scale,  $\Omega$ . At the fixed point, the energy scale is give by  $\Omega \sim L^{-z}$  if only a small fraction  $1/L$  of sites is active (i.e. not yet decimated). In our computations we consider finite periodic chains with  $L = \text{even}$  sites and decimate until the last pair of sites having a gap  $\Delta \sim \Omega$ . From the distribution of the logarithms of the gap:

$$P(\ln \Delta) \sim \Delta^{1/z}, \quad \Delta \rightarrow 0, \quad (10)$$

we obtain the the dynamical exponent,  $z$ . In the random singlet phase, the dynamical exponent is formally infinite, as described in eq.(2), and the appropriate scaling combination in a finite system is given by:

$$\ln [L^\psi P(\ln \Delta)] \simeq f(L^{-\psi} \ln \Delta). \quad (11)$$

The SDRG method as outlined above is expected to provide asymptotically exact results both in the RS phase<sup>6</sup> and in the Griffiths region.<sup>17</sup>

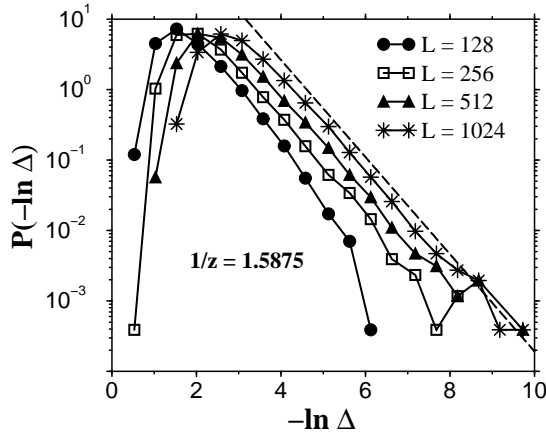


Fig. 1. Test of the SDRG method on random dimerized  $XX$ -chains, with  $\alpha = 0.6, x = 0.6$ . The slope of the distribution of the gaps in a log-log scale agrees well with the known exact result for the dynamical exponent, which is given by the slope of the broken straight line.

In the present model the randomness is discrete and at the starting point of the renormalization there are several couplings with the same value of  $\Omega$ . In this degenerate situation we randomly choose the actual coupling to be decimated. After a sufficiently large number of renormalization steps we will have a (quasi)continuous distribution. To illustrate the correctness of the SDRG procedure for discrete randomness, we consider the random dimerized  $XX$ -chain<sup>19</sup> in which the couplings take the value  $J$  or  $\alpha J$  and a fraction,  $x$ , of the odd (even) couplings are  $J$  ( $\alpha J$ ). To be close to our model in eq.(8) we took  $\alpha = 0.6$  and  $x = 0.6$  for the  $XX$ -chain. In Fig. 1 the distribution of the gaps for different finite systems is shown in a log-log scale, the asymptotic slope of which

agrees very well with the known *exact* result<sup>18</sup> for  $1/z$  which is given by the formula  $[(J_e/J_o)^{(1/z)}] = 1$ , i.e. by the solution of the equation  $(xJ^{(1/z)} + (1-x)(\alpha J)^{(1/z)}) \cdot ((1-x)J^{(-1/z)} + x(\alpha J)^{(-1/z)}) = 1$ .

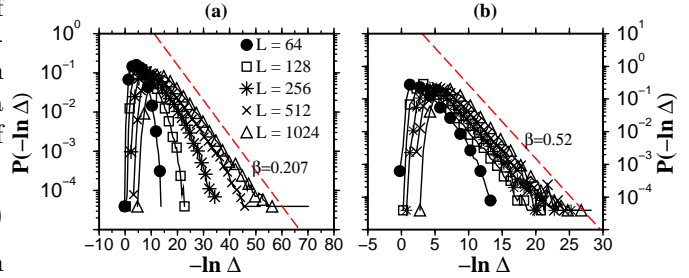


Fig. 2. Distribution of the energy gap for the fixed parity model for two concentrations:(a)  $x = 0.6$ , (b)  $x = 0.8$ . The asymptotic slope of the curves, indicated by broken straight lines, gives the susceptibility exponent,  $\beta$ .

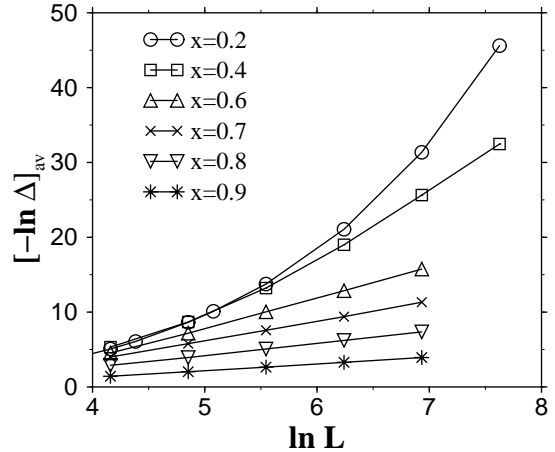


Fig. 3. Average gap of the fixed parity model with different concentrations,  $x$ , as a function of the size,  $L$ . The asymptotic slope of the curves in log-log scale defines the dynamical exponent,  $z = 1/\beta$ . Note the strong finite size corrections: for sizes used in DMRG ( $\ln L \leq 5$ ) we are not in the asymptotic regime.

### 3.2 Fixed parity model

Next, we turn to our model defined in eq. (8) and start with the fixed parity case. The distribution of the gaps for two different values of the concentration,  $x = 0.6$  and  $0.8$ , are shown in Fig. 2. Evidently, the exponent  $\beta$ , given by the asymptotic slope of the distributions, is finite and concentration dependent. It can also be extracted from the scaling behavior of the average gap via  $[\ln \Delta]_{\text{av}} \simeq \text{const} + \beta^{-1} \ln L$ . As seen in Fig. 3 one can obtain a reliable estimate of  $\beta$  for  $x \geq 0.4$ . For smaller concentrations, even the largest system size  $L = 2048$  is not yet in the asymptotic regime. The estimates for

$\beta$  are depicted in Fig. 4. They are systematically lower than the DMRG results in ref. 12, which is probably due to finite-size effects. Using the DMRG method, ref. 12 reports results up to  $\ln L \leq 5$ , which is, even for comparatively large concentrations, not in the asymptotic regime according to Fig. 3.

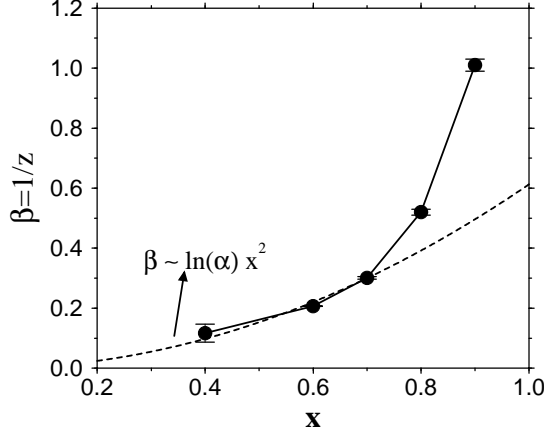


Fig. 4. The susceptibility exponent,  $\beta = 1/z$ , for the fixed parity model as a function of the concentration. For small  $x$  the expected quadratic dependence is denoted by the dotted curve.

As can be seen in Fig. 4, for small concentrations there is a quadratic dependence:  $\beta \sim x^2$ , which can be understood as follows: In the fixed parity model the average value of the log-couplings in the odd and even positions are different, so that the dimer control parameter in eq. (3) is  $\delta \sim x^2 \ln \alpha \neq 0$ . For small  $x$ , thus for small  $\delta$  we can use eq. (5), which is compatible with the observed quadratic  $x$ -dependence of  $\beta$ .

### 3.3 Random parity model

For the random parity model the gap distribution for an intermediate concentration,  $x = 0.8$ , is shown in Fig. 5(a). One observes that the distribution gets systematically broader with increasing system size, which is a characteristic of the RS phase. Indeed, the logarithmic scaling in eq. (11) is well satisfied with  $\psi = 1/2$ , as illustrated in Fig. 5(b). The same logarithmic scaling with  $\psi = 1/2$  holds for other values of the concentration, too. These results can be understood by noting that odd and even couplings have on average of the same strength in the random parity model, consequently the (dimer) control parameter is  $\delta = 0$ . The short-range correlations in the dimerized sequences, especially for large concentration, does not modify this large-scale asymptotic behavior. Our results for the random parity model are in agreement with the DMRG calculations in ref. 12.

### 3.4 Correlated random parity model

Now we discuss the results for the correlated random parity model. We recall that according to scaling arguments<sup>13,20</sup> the disorder correlations modify the critical behavior in the RS phase, provided the decay exponent

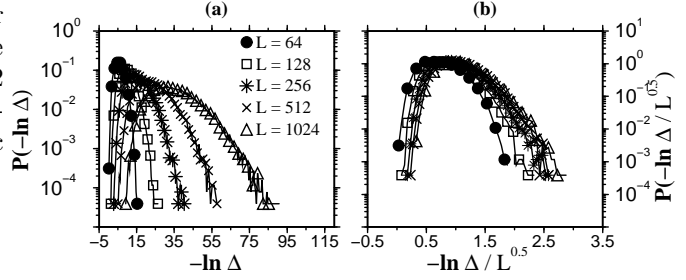


Fig. 5. Probability distribution of the gaps in the random parity model with  $x = 0.8$  (a). Scaling collapse for different sizes using the scaling form in eq.(11) (b).

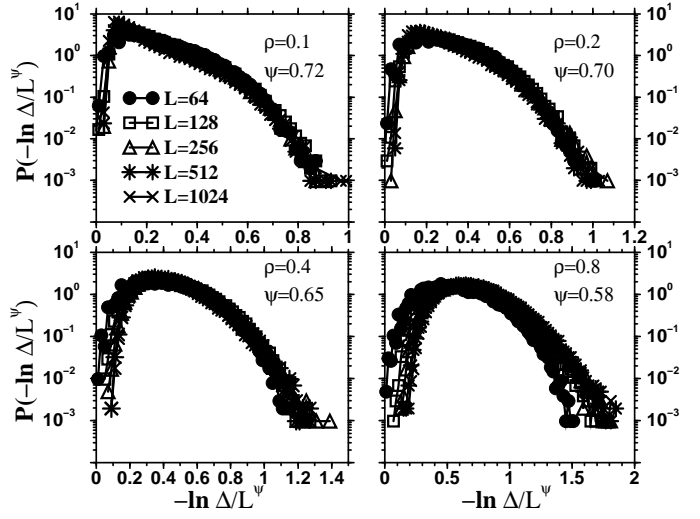


Fig. 6. Scaling plot of the gap distribution for the correlated random parity model for different values of  $\rho < 1$ . The  $\psi$  exponent is  $\rho$ -dependent and well described by the relation in eq.(12).

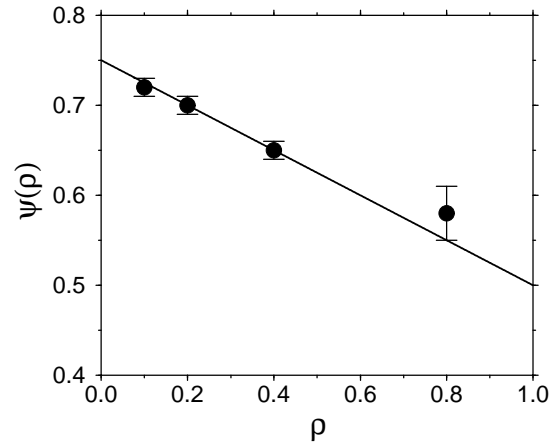


Fig. 7. Variation of the estimated exponents  $\psi(\rho)$  for the correlated random parity model with the correlation parameter  $\rho$ . The solid line represents the linear fit in Eq.(12).

is sufficiently small:  $\rho < 2/\nu$ , where  $\nu = 2$  is the correlation length exponent for uncorrelated disorder. To illustrate this relation we estimate the control parameter,  $\delta$ , in a finite chain of length,  $L$ . Introducing the notation  $\epsilon_i = \ln(J_{2i}/J_{2i-1})$ , we have  $\delta^2 = 1/4L^2 \left[ \left( \sum_{i=1}^{L-1} \epsilon_i \right)^2 \right] \sim 1/L \int_1^L G(r) dr \sim L^{-\rho}$ , where  $G(r)$  is the disorder correlator. Thus  $\delta \sim L^{-\rho/2}$ , for  $\rho < 1$ , whereas for  $\rho \geq 1$  we have the non-correlated disorder result,  $\delta \sim L^{-1/2}$ . We can conclude from this consideration that for  $\rho < 1$  the correlated random parity model has a vanishing gap and is in the RS phase, however with  $\rho$ -dependent properties. The scaled gap distribution for four different correlation parameters,  $\rho < 1$ , is shown in Fig. 6, in which the logarithmic scaling collapse in eq. (11) can be obtained with different exponents,  $\psi(\rho)$ . A plot of the  $\psi(\rho)$  data is given in Fig. 7 in which the  $\rho$  dependence can be well fitted with the approximate formula:

$$\psi(\rho) = \frac{3-\rho}{4}, \quad \rho < 1. \quad (12)$$

This result is exact at  $\rho = 1$ , in which case the standard, non-correlated RS phase result,  $\psi = 1/2$  is recovered. For a small  $\rho$  the exponent approaches  $\psi \approx 3/4$ , but at  $\rho = 0$  we jump to the fixed parity model. The linear dependence of  $\psi(\rho)$  on  $\rho$  in eq.(12) is in the same form as in the exact expression for the  $XX$ -model<sup>13</sup> with correlated randomness.

The low-temperature singularity of the susceptibility of the correlated random parity model is given by the formula:

$$\chi(T) \sim \frac{1}{T(\ln T)^{1/\psi}}, \quad (13)$$

in which  $\psi$  is  $\rho$ -dependent, as given in Eq.(12).

#### 4. Discussion

We close our paper by comparing the experimentally measured low-temperature susceptibility of the compound  $\text{CuCl}_{2x}\text{Br}_{2(1-x)}(\gamma - \text{pic})_2$  with the results of our theoretical calculations. We recall that the measured susceptibility exponent is finite,  $\beta_{\text{exp}} \approx 0.5 - 0.67$ , and has only a weak concentration dependence. These properties are partially compatible with the results for the fixed parity model, which is found to be in the Griffiths phase, where  $\beta$  is finite for all values of the concentration. According to Fig. 4 there is a range of concentration around  $x \approx 0.8$  in which our results for  $\beta$  agree with the experimental values. However, this range is rather narrow and our values for  $\beta$ , which have a substantial concentration dependence, are generally significantly smaller than  $\beta_{\text{exp}}$ . For models with non-strictly correlated parities, in which case  $\beta$  is found formally zero, the agreement with the experiment is even less satisfactory. One possible explanation of this discrepancy between experiment and theory is that the experimentally measured  $\beta_{\text{exp}}$  are effective, temperature dependent values, which should approach the true behavior as  $T \rightarrow 0$ . Indeed, as seen in Fig. 3 the local slopes of the curves that show  $\ln \Delta$  vs.  $\ln L$ , which define the effective exponent  $z(L) = 1/\beta(L)$ , have a strong size dependence. This can be converted into a temperature dependence through  $\Omega \sim T \sim L^{-z}$ .

The corrections to  $\beta(L)$  are particularly strong for small values of  $x$ . For moderately large sizes,  $\ln L \approx 5$ , the effective exponents have only a weak concentration dependence. The leading finite size corrections are of the form,  $\beta(L) \simeq \beta + a/L$ , which are compatible with a temperature correction as:

$$\beta(T) \simeq \beta + cT^\beta + \dots \quad \beta > 0., \quad (14)$$

In the random singlet phase with  $\beta = 0$ , both for correlated and non-correlated parity, the effective exponents have a logarithmic temperature dependence:

$$\beta(T) \simeq \frac{c_1}{|\ln T|} + \dots \quad \beta = 0., \quad (15)$$

which can be obtained by analyzing eqs.(6) and (13). Indeed, these finite temperature corrections are strong for the fixed parity model, particularly for small  $\beta$ , i.e. for a small concentration,  $x$ .

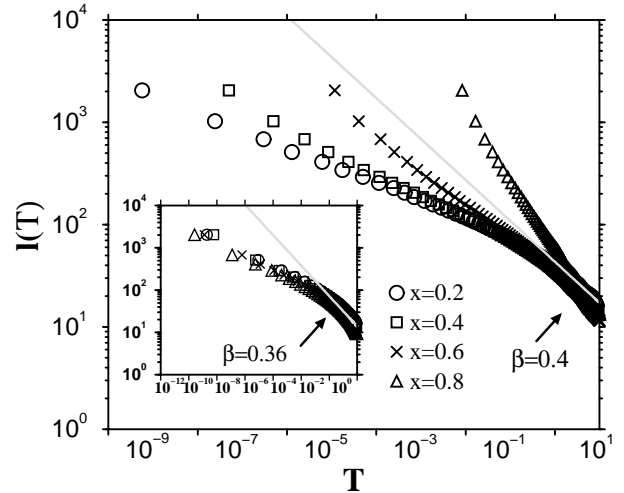


Fig. 8. Temperature dependent length-scale,  $l(T)$ , which is obtained by performing the renormalization down to an energy  $\Omega = T$ , for the fixed parity and the random parity (inset) models. In the log-log plot the local slope of the curves gives the temperature dependent effective exponent,  $\beta(T)$ . The slope of the straight line indicates the effective exponent at  $T = 2\text{K}$ .

We tried to estimate the effective exponent,  $\beta(T)$ , at the temperature of the experimental measurement  $T = 2\text{K}$ . For this we performed the renormalization transformation down to an energy-scale,  $\Omega = T$ , and measured the fraction of non-decimated sites:  $n(\Omega) = 1/l(\Omega)$ . Here the length-scale is given by  $l(\Omega) \sim \Omega^{-\beta}$ . Our results for  $l$  as a function of the temperature for the fixed parity and the random parity model are presented in Fig. 8 for different values of the concentration. In the log-log plot the local slope of the curves is just the effective exponent,  $\beta(T)$ , at  $T = \Omega$ . As can be seen in this figure the effective exponent,  $\beta(T)$ , approaches its limiting value only if the temperature is sufficiently low. At the temperature of the measurement,  $T = 2\text{K}$ , the asymptotic region seems to be still quite far. For the fixed parity model the effective exponent is about  $\beta = 0.4$ , which is prac-

tically independent of the concentration. This result is consistent with the experimental results of ref. 9. For the random parity model, as shown in the inset, the effective exponent continuously vary with the temperature. Its value at  $T = 2\text{K}$  is about  $\beta = 0.36$ , which is also consistent with the experiments. Therefore, using the available experimental data it is not possible to distinguish the type of parity correlations present in the compound,  $\text{CuCl}_{2x}\text{Br}_{2(1-x)}(\gamma - \text{pic})_2$  and the question, which type of model should be used for its theoretical description remains still open. Experimental measurements at lower temperatures are needed to clarify this point.

### Acknowledgment

This work has been supported by a German-Hungarian exchange program (DAAD-MÖB), by the Hungarian National Research Fund under grant No OTKA TO34138, TO37323, MO45596 and M36803, by the Ministry of Education under grant No. FKFP 87/2001 and by the Centre of Excellence ICA1-CT-2000-70029.

- 1) A. Luther and I. Peschel, Phys. Rev. B **12** (1975) 3908.
- 2) M.C. Cross and D.S. Fisher, Phys. Rev. B **19** (1979) 402.
- 3) For a review see e.g.: H. Rieger and A.P. Young, *Quantum Spin Glasses*, Lecture Notes in Physics **492**, in "Complex Behaviour of Glassy Systems", p. 254, ed. J.M. Rubi and C. Perez-Vicente (Springer Verlag, Berlin-Heidelberg-New York, 1997).
- 4) R.B. Griffiths, Phys. Rev. Lett. **23** (1969) 17.
- 5) B. McCoy, Phys. Rev. Lett. **23** (1969) 383.
- 6) D.S. Fisher, Phys. Rev. B **50** (1994) 3799.
- 7) S.K. Ma, C. Dasgupta, and C.-K. Hu, Phys. Rev. Lett. **43** (1979) 1434; C. Dasgupta and S.K. Ma, Phys. Rev. B **22** (1980) 1305.
- 8) R.A. Hyman, K. Yang, R.N. Bhatt, and S.N. Girvin, Phys. Rev. Lett. **76** (1996) 839.
- 9) Y. Ajiro, T. Wakisaka, H. Itoh, K. Watanabe, H. Satoh, Y. Inagaki, T. Asano, M. Mito, K. Takeda, H. Mitamura, and T. Goto, Physica B **329-333** (2003) 1004.
- 10) T. Wakisaka, Master Thesis (Kyushu University), (2003).
- 11) H.J.M. de Groot, L.J. de Jongh, and R.D. Willett, J. Appl. Phys. **53** (1982) 8038.
- 12) K. Hida, J. Phys. Soc. Jpn. **72** (2003) 2627.
- 13) H. Rieger and F. Iglói, Phys. Rev. Lett. **83** (1999) 3741.
- 14) Y.-C. Lin, N. Kawashima, F. Iglói and H. Rieger, Prog. Theor. Phys. (Suppl.) **138** (2000) 470; D. Karevski, Y.-C. Lin, H. Rieger, N. Kawashima and F. Iglói, Eur. Phys. J. B **20** (2001) 267.
- 15) R. Mélin, Y.-C. Lin, P. Lajkó, H. Rieger, and F. Iglói, Phys. Rev. B **65** (2002) 104415.
- 16) Y.-C. Lin, R. Mélin, H. Rieger and F. Iglói, Phys. Rev. B **68** (2003) 024424.
- 17) F. Iglói, R. Juhász, and P. Lajkó, Phys. Rev. Lett. **86** (2001) 1343.
- 18) F. Iglói, R. Juhász, and H. Rieger, Phys. Rev. B **61** (2000) 11552.
- 19) For the random  $XX$  model the decimation rule in Eq.(9) is modified by having a prefactor 1 instead of  $1/2$ .
- 20) A. Weinrib, and B.I. Halperin, Phys. Rev. B **27** (1983) 413.